UC Davis
UC Davis Previously Published Works

Title

Nonequilibrium gating and voltage dependence of the ClC-0 Cl- channel.

Permalink

Journal

ISSN

Authors

Chen, TY
Miller, C

Publication Date

DOI

Peer reviewed

Nonequilibrium Gating and Voltage Dependence of the ClC-0 Cl⁻ Channel

TSUNG-YU CHEN and CHRISTOPHER MILLER

From the Howard Hughes Medical Institute, Graduate Department of Biochemistry, Brandeis University, Waltham, Massachusetts 02254

ABSTRACT   The gating of ClC-0, the voltage-dependent Cl⁻ channel from *Torpedo* electric organ, is strongly influenced by Cl⁻ ions in the external solution. Raising external Cl⁻ over the range 1–600 mM favors the fast-gating open state and disfavors the slow-gating inactivated state. Analysis of purified single ClC-0 channels reconstituted into planar lipid bilayers was used to identify the role of Cl⁻ ions in the channel's fast voltage-dependent gating process. External, but not internal, Cl⁻ had a major effect on the channel's opening rate constant. The closing rate was more sensitive to internal Cl⁻ than to external Cl⁻. Both opening and closing rates varied with voltage. A model was derived that postulates (*a*) that in the channel's closed state, Cl⁻ is accessible to a site located at the outer end of the conduction pore, where it binds in a voltage-independent fashion, (*b*) that this closed conformation can open, whether liganded by Cl⁻ or not, in a weakly voltage-dependent fashion, (*c*) that the Cl⁻-liganded closed channel undergoes a conformational change to a different closed state, such that concomitant with this change, Cl⁻ ion moves inward, conferring voltage-dependence to this step, and (*d*) that this new Cl⁻-liganded closed state opens with a very high rate. According to this picture, Cl⁻ movement within the pre-open channel is the major source of voltage dependence, and charge movement intrinsic to the channel protein contributes very little to voltage-dependent gating of ClC-0. Moreover, since the Cl⁻ activation site is probably located in the ion conduction pathway, the fast gating of ClC-0 is necessarily coupled to ion conduction, a nonequilibrium process.

KEY WORDS: chloride channel • ClC-0 • gating • voltage dependence

INTRODUCTION

Integral membrane proteins spend their lives in the presence of high electric fields, 10^7–10^8 V/m, close to the dielectric breakdown limit of bulk matter. All charged residues in the transmembrane domains of such proteins are thus subjected to large electrostatic forces. Many ion channel proteins have evolved not merely to survive in these fields, but to exploit them. "S4-type" voltage-gated Na^+, K^+, and Ca^{2+} channels, for example, use transmembrane voltage to drive physiologically meaningful conformational changes (Sigworth, 1994). For these channels, it is widely agreed (despite a paucity of direct evidence) that much of the charge that confers voltage dependence upon the gating process resides in the positively charged S4 transmembrane sequence, a motif dense in arginine and lysine residues unique to these proteins. Recent work (Larsson et al., 1996; Yang et al., 1996) argues that when these channels open, the S4 sequence moves outward, carrying its cargo of positively charged residues. This channel family provides the clearest picture of intrinsic voltage dependence of gating, in which the conformational changes leading to the open state involve physical movements of charged residues through the transmembrane voltage gradient.

In contrast, little is understood about the gating mechanisms of voltage-dependent Cl⁻ channels, which are found in nerve and muscle cells as well as in many types of inexcitable tissues (Pusch and Jentsch, 1994; Jentsch et al., 1995). A large molecular family of Cl⁻ channels is currently being uncovered in the wake of the cloning of its founding member, ClC-0, from the electric organ of the *Torpedo* ray (Jentsch et al., 1990; O'Neill et al., 1991). These "ClC"-type channels carry out a variety of physiological tasks. The ClC-0 channel, working in concert with the nicotinic acetylcholine receptor, allows the electroplax to act as a high-current underwater stun-gun (Miller and White, 1980). A homologous channel, ClC-1 (Steinmeyer et al., 1991*b*), controls the resting membrane potential and excitability of mammalian skeletal muscle, and certain inherited myotonias in goats, mice, and humans are caused by its disruption (Bryant and Morales-Aguilera, 1971; Palade and Barchi, 1977; Steinmeyer et al., 1991*a*; George et al., 1993; Steinmeyer et al., 1994). Another such channel, ClC-2, expressed ubiquitously in mammalian tissues, is sensitive to osmotic strength (Grunder et al., 1992; Thiemann et al., 1992) and may be involved in cell volume regulation. Recently, disruption of the ClC-5 gene has been identified as the cause

Address correspondence to Dr. Christopher Miller, Howard Hughes Medical Institute, Graduate Department of Biochemistry, Brandeis University, Waltham, MA 02254. Fax: 617-736-2365; E-mail: cmiller@binah.cc.brandeis.edu

of several types of human familial kidney stone diseases (Lloyd et al., 1996). Within the ClC family, only ClC-0 has been studied in functional detail at both the macroscopic and single-channel levels (Miller and Richard, 1990; Pusch and Jentsch, 1994).

The gating of ClC-0 is influenced by voltage in an apparently conventional way in which depolarization speeds opening and slows closing rates (Miller, 1982; Hanke and Miller, 1983). But the channel is unusual in that its gating also responds to Cl^- ion, via both the transmembrane Cl^- gradient and the absolute concentration of external Cl^- (Richard and Miller, 1990; Pusch et al., 1995). ClC-0 is, in effect, a voltage-gated, Cl^--activated Cl^- channel. External Cl^- acts as an activating ligand, such that the Cl^--occupied channel is more likely to open than is the unoccupied channel. The issue concerning us here is the coupling between voltage and Cl^- activation. Pusch and colleagues (1995) recently proposed a specific mechanism for this coupling. According to their picture, the Cl^--activation site resides deep within the conduction pore itself, accessible to external (but not internal) Cl^- in the channel's closed state. The voltage dependence of channel opening thus arises from the voltage dependence of Cl^- binding, not from an intrinsically voltage-dependent conformational change. This proposal rationalizes the absence in ClC channels of an S4-like sequence and offers a framework for understanding the coupling of gating to transmembrane flow of Cl^- (Richard and Miller, 1990).

Pusch and co-workers (1995) provided compelling evidence that the Cl^--activation site is located in the conduction pathway, but they did not experimentally address the mechanism by which Cl^- acts. It is our intention here to test the above idea quantitatively in hopes of identifying the source of voltage-dependent gating in ClC-0. Are the opening and closing rates of the channel intrinsically voltage dependent, as in S4-type channels, or is it the binding of activator Cl^- that confers voltage dependence upon these rates? By examining the kinetics of single ClC-0 channels, we demonstrate that gating is dominated by voltage-sensitive opening and closing rates, with binding of external Cl^- having little or no voltage dependence. However, the voltage sensitivity of gating is not due to charges built into the protein structure; rather, it arises from Cl^- ion in the pore traversing the transmembrane voltage drop during conformational changes preceding channel opening.

MATERIALS AND METHODS

Materials

All chemicals used were reagent grade. Phospholipids were obtained from Avanti Polar Lipids, (Alabaster, AL). For liposome reconstitution, phosphatidylcholine (PC), phosphatidylethanolamine (PE), and phosphatidylserine (PS) were from bovine brain, while for planar bilayer recording, 1-palmitoyl, 2-oleoyl forms of the phospholipids were used (POPC, POPE, respectively). Cholesterol and ergosterol were from Sigma Chemical Co. (St. Louis, MO) and were recrystallized from ethanol. Nystatin (Fluka, Ronkonkoma, NY) was prepared each week as a 1 mg/ml stock solution in methanol. All lipid and nystatin solutions were stored at $-70°C$. Electric rays, *Torpedo californica*, were obtained live from Aquatic Research Consultants (San Pedro, CA). In biochemical preparations of ClC-0 channels, we used a "lipid mix" containing PE/PC/PS/cholesterol or ergosterol, 5/1/2/2 (mole fraction).

Purification and Liposome Reconstitution of ClC-0

Light vesicles from the noninnervated-face membranes of *T. californica* electrocytes were prepared on sucrose density gradients as described (Hanke and Miller, 1983) and were stored in aliquots at $-70°C$. The functionally active channel protein was purified to single-band homogeneity by immunoaffinity methods, as documented in detail (Middleton et al., 1994a,b). Briefly, light vesicles were solubilized in "buffer 1" (125 mM NaCl, 25 mM KCl, 10 mM glutamic acid, 0.5 mM EGTA, and 20 mM Tris-HCl, pH 7.6) containing 25 mM CHAPS. After incubation on ice for 30 min, insoluble material was removed by centrifugation at 100,000 g in a Ti 70.1 rotor (Beckman Instruments, Inc., Brea, CA) for 30 min. Solubilized protein was incubated with immunoaffinity resin for 30 min, the flow-through being drained subsequently. The immunoaffinity column was washed with 5 column volumes of buffer 1 containing 15 mM CHAPS and 0.1 mg/ml lipid mix, and then with 5 column volumes of buffer 1 containing 0.1% Triton X-114 and 0.1 mg/ml lipid mix. Pure ClC-0 protein was eluted with buffer 1 containing 15 mM CHAPS, 0.1 mg/ml lipid mix, adjusted to pH 11.2 with NaOH, and was quickly neutralized to ~pH 7.5 with 1 M HCl. The presence and purity of ClC-0 channel in the final eluate was later assessed by silver-stained PAGE gels and by Western blots probed with anti-ClC-0 antibody (Middleton et al., 1994b).

Proteoliposomes reconstituted with ClC-0 protein were prepared as follows: To buffer 1 containing 15 mM CHAPS, lipid mix (PE/PC/PS/ergosterol, 5/1/2/2) was added to a final concentration of 2 mg/ml. To this solution, purified ClC-0 was added to the desired concentration (2–10 μg/ml). In order to obtain reliably only a single channel in the planar bilayer, the protein/lipid ratio was adjusted empirically so that the average number of channels per fusion event was less than one. After a 30-min incubation on ice, detergent was removed by centrifuging through Sephadex G-50 columns (100 μl sample for a 1.5 ml column), as described previously (Middleton et al., 1994b). Proteoliposomes were stored in 120-μl aliquots at $-70°C$ for up to 8 wk.

Planar Bilayer Recording of Reconstituted ClC-0 Channels

All channel recordings were made after incorporation of ClC-0 channels into planar lipid bilayers formed from POPE/POPC (16 mg/ml and 4 mg/ml, respectively, in n-decane). The planar bilayer system has been described in detail (Neyton and Miller, 1988), except for an innovation essential for these experiments. We constructed a horizontal bilayer chamber using a partition formed from a plastic cover-slip separating an "upper" from a "lower" aqueous chamber. Bilayers were cast on a 60–100 μm diameter hole formed in the partition by the "melt-shave" method (Wonderlin et al., 1990). Bilayer solutions were 5 mM tris-glutamate, pH 7.4, with the desired concentration of NaCl and Na-glutamate. Both aqueous chambers (0.3–0.5 ml volume) could be perfused for convenient solution changes (exchange

time ~15 s). The chambers were connected to an Axopatch 200-A amplifier via salt bridges containing 300 mM Na-glutamate. Bilayer formation was followed visually under a dissecting stereo-microscope and electrically by continuous capacitance measurement. Planar bilayers were typically in the range of 50–80 pF capacitance and >100 GΩ resistance.

Single reconstituted ClC-0 channels were incorporated into the planar bilayers by the "nystatin-spike" method (Woodbury and Miller, 1990), in which fusion of ergosterol-containing proteoliposomes with the planar bilayer is promoted by the ionophore nystatin in the presence of a salt gradient. An aliquot of ClC-0 proteoliposomes was thawed at room temperature and then immediately re-frozen and thawed 1–2 times more. Nystatin (10–20 μg/ml final concentration) was added, and the sample was sonicated for 1–2 s in a cylindrical bath sonicator. An additional 200 mM NaCl was added to the sonicated proteoliposomes to increase the density of the solution. (Final salt concentration in the liposome suspension was ~360 mM.) For each attempt at channel incorporation, 0.5–1 μl of sample was allowed to settle directly onto the horizontal planar bilayer, with bilayer solutions containing 150 and 15 mM NaCl in the upper and lower chambers, respectively. If a ClC-0 channel (recognized by its characteristic double-barreled gating behavior) failed to appear in the bilayer within 3 min, the process was repeated, usually with a new bilayer. As soon as a single ClC-0 channel appeared in the bilayer, the lower chamber was perfused with a solution of the same ionic strength as that in the upper chamber, to remove the salt gradient and thus suppress further liposome fusion. Most ClC-0 channels inserted with the cytoplasmic side facing the upper chamber, as could be easily determined by the polarity of voltage activation. Henceforth, we use the electrophysiological convention to refer to channel sidedness, with the external side of the channel defined as electrical ground. For measurements of macroscopic ClC-0 currents in bilayers containing many channels, we fused sucrose-loaded *Torpedo* electroplax plasma membrane vesicles directly into the bilayer without applying a salt gradient or nystatin (Miller and White, 1980). Since our experiments required variation of Cl$^-$ concentration over a wide range (1–600 mM), we customarily maintained ionic strength with Na-glutamate.

Electrophysiological measurements were controlled by a Microstar DAP 3200e acquisition board installed in a 486 computer using home-written software. Single-channel records were Bessel-filtered (140 Hz corner frequency) and sampled at 1 kHz. In off-line analysis, a digital gaussian filter was further applied to the data, such that the final equivalent corner frequency was 100 Hz.

Analysis of Single-channel Records

The ClC-0 channel displays an unusual and delightful gating behavior that must be taken into account for the analysis used here. As illustrated in the single-channel traces shown in Fig. 1, the channel gates in bursts of millisecond timescale opening-closing transitions separated by long-lived, zero-conductance "inactivated" intervals. The burst itself shows three equally spaced conductance levels, labeled 0, 1, and 2. These are known to reflect the "double-barreled" nature of ClC-0 (Miller, 1982; Hanke and Miller, 1983; Bauer et al., 1991); the channel contains two identical Cl$^-$ diffusion pores which open and close independently of one another. We are concerned here with the fast gating process, and so the long-lived inactivation events must be eliminated in the analysis. At relatively depolarized membrane potentials, as in Fig. 1 A, the "state-0" closed events within a burst and the inactivation events that separate bursts can be easily distinguished from their very different dwell-time distributions. After elimination of inactivation events by eye, the dwell-time histograms (Fig. 1 A, *right*) reveal that each of the three levels within the burst follows a single exponential distribution. The time constants of these distributions, τ_i, were used to determine the fundamental opening and closing rate constants, α and β, respectively, of each individual pore (Hanke and Miller, 1983; Miller and Richard, 1990):

$$1/\tau_0 = 2\alpha, \tag{1a}$$

$$1/\tau_1 = \alpha + \beta, \tag{1b}$$

$$1/\tau_2 = 2\beta, \tag{1c}$$

Moreover, the fundamental probability of channel opening p_o is given, via the binomial distribution of the observed state-probabilities, f_i:

$$p_o = f_1/2 + f_2. \tag{1d}$$

Thus, the fundamental gating rate constants α and β are overdetermined from the measured dwell-times and state-probabilities. For this reason, we were usually able to check our rate constant determinations for internal consistency, according to two separate measurements for each:

$$\alpha = 1/(2\tau_0), \tag{2a}$$

$$\alpha = p_o/\tau_1, \tag{2b}$$

$$\beta = 1/(2\tau_2), \tag{2c}$$

$$\beta = (1 - p_o)/\tau_1. \tag{2d}$$

However, at strongly hyperpolarized membrane potentials, as in Fig. 1 B, the inactivation events shorten and the closed times lengthen, so that it becomes difficult to separate the two types of nonconducting dwell-times. Under such conditions, the dwell-times in states 1 and 2 are still exponentially distributed, but the nonconducting dwell-times follow double-exponential distributions (Fig 1 B, *right*). Because our analysis depends crucially upon the opening rate at hyperpolarized potentials, it is essential to avoid contamination of the fast gating process by brief inactivation events. Under these conditions, values of f_1, f_2, and τ_0 vary with the subjectively chosen inactivation-time cutoff, and so neither p_o, α, nor β can be objectively measured in the usual way.

We circumvent this difficulty by exploiting the fact that measured values of τ_1 and τ_2, and the ratio f_2/f_1, are completely independent of the inactivation time. Thus, under conditions of ambiguity between closed and inactivated times (e.g., hyperpolarized voltages), we can measure the basic gating parameters without reference to closed-state values. To do this, we use Eqs. 2b and 2d in combination with an open-probability defined by:

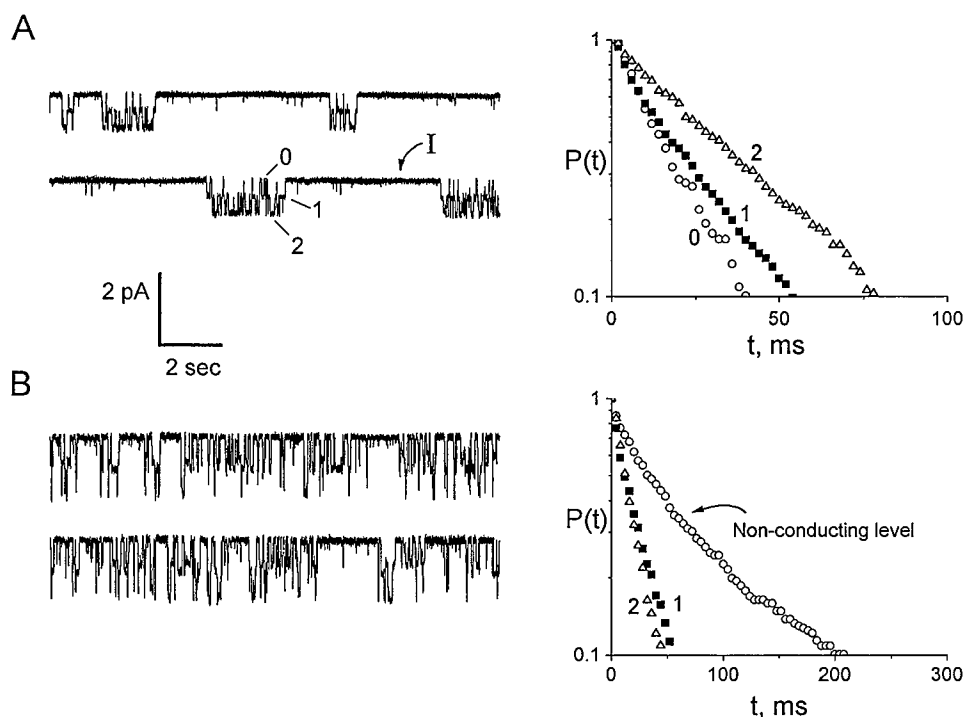$$p_o = 2\sigma/(1 + 2\sigma), \tag{3}$$

where $\sigma = f_2/f_1$.

A

B

FIGURE 1. Fast and slow gating of single ClC-0 channels. Single ClC-0 channels were recorded in solutions containing 4 mM $[Cl^-]_{ex}$ and 150 mM $[Cl^-]_{in}$. (*A, left*) Recording at a relatively depolarized membrane potential (−20 mV) at which closed events and inactivation events can be readily separated by eye. (*right*) Cumulative dwell-time distributions for conductance levels 0 (○), 1 (■), and 2 (△), after long-lived inactivation events were removed subjectively. (*B, left*) Recording taken from the same channel at a relatively hyperpolarized membrane potential (−70 mV), where inactivation and closed dwell-times are not easily separated. (*right*) Dwell-time distributions as in *A*, except that no attempt was made to exclude inactivation events from the nonconducting dwell-times.

In this way α and β become independent of the criteria used to eliminate inactivation events. Table I compares the channel parameters calculated from these two different methods, at voltages where we can unambiguously remove inactivation events (as in Fig 1 *A*). Values of p_o, α, and β obtained by these two methods agree within 10%. Furthermore, f_0, f_1, and f_2 follow the binomial distribution demanded by the two-pore picture of the channel, as has been confirmed repeatedly in the past (Hanke and Miller, 1983; Miller and Richard, 1990) and is required for valid use of Eq. 3. We have also established (not shown) that in cases in which closed and inactivated events are not readily separable, the parameters calculated from two different methods agree if the inactivation time cutoff is chosen to force a binomial distribution of the state-probabilities. All data presented here were calculated using this method.

Missed Events Correction

The conductance of each pore in a ClC-0 channel is ~10 pS in symmetrical 150 mM Cl⁻, corresponding to ~0.5 pA at −50 mV. This small current amplitude necessitates the use of a heavy low-pass filter (100 Hz corner frequency), which makes events of <1.8-ms duration undetectable. We corrected for these missed events by simulating ideal records for two independently gating pores, with varying opening and closing rates at different channel open probabilities. These idealized records were passed through the same filter as the experimental records. Empirical curves were constructed to correct the observed time constants for the effects of missed events. In the worst cases (at the two extremes of the voltage range in high $[Cl^-]_{ex}$), the observed opening and closing rates were ~6% lower than the corrected values.

TABLE I

Comparison of Channel Parameters Calculated by Two Different Methods

V	p_o A	p_o B	α, s^{-1} A	α, s^{-1} B	β, s^{-1} A	β, s^{-1} B	f_0	f_1	f_2
mV									
−10	0.78	0.77	39.7	36.1	11.4	10.6	0.042 (0.048)	0.355 (0.342)	0.603 (0.610)
−20	0.70	0.69	27.5	27.2	13.7	12.1	0.091 (0.093)	0.428 (0.424)	0.481 (0.483)
−30	0.62	0.62	26.5	23.6	14.0	14.7	0.143 (0.145)	0.475 (0.471)	0.382 (0.384)
−40	0.55	0.55	19.8	20.8	15.7	16.8	0.201 (0.201)	0.494 (0.495)	0.305 (0.305)

The table gives an example of the agreement between single-channel gating parameters calculated by two different methods, under conditions where closed and inactivated events could be unambiguously separated. A single channel was recorded (at 4 and 150 mM external and internal Cl⁻, respectively) at the indicated voltages, and dwell-times in the three states were compiled. Inactivation events were removed by excluding from the analysis all nonconducting events longer than a subjectively chosen cutoff-time. The state-probabilities, f_i, were then calculated. In Method A, rate constants, α and β, and open-probability, p_o, were calculated according to Eqs. 2a, 2c, and 1d, respectively. In Method B, the same parameters were calculated according to Eqs. 2b, 2d, and 3, which ignore all data from nonconducting levels. The state-probabilities predicted from a binomial distribution are also shown in parentheses.

It is a truth universally acknowledged that single-channel behavior provides mechanistic information that is often lost in the ensemble-averaging of macroscopic experiments. But it has been technically difficult to obtain single ClC-0 channels for routine gating analysis, for several reasons. *Torpedo* electrocytes, the natural source, contain a very high density ($\sim$1000/μm^2) of ClC-0 in their plasma membranes (White and Miller, 1979; Miller and White, 1980; Goldberg and Miller, 1991). Even when expressed at low density in various heterologous systems, the channels tend to cluster into high-density rafts, and membrane patches sampled from such cells display either many channels or none (Bauer et al., 1991). We circumvented this problem by purifying ClC-0 channels from *Torpedo* electroplax and reconstituting them into planar lipid bilayer membranes. This approach provides a way to disperse the channels in lipid-detergent micelles at an experimentally adjustable density, and thus routinely achieve recordings containing only a single channel (Woodbury and Miller, 1990; Middleton et al., 1994*a*). A silver-stained gel of the purified ClC-0 preparation used here is shown in Fig. 2; the active channel com-
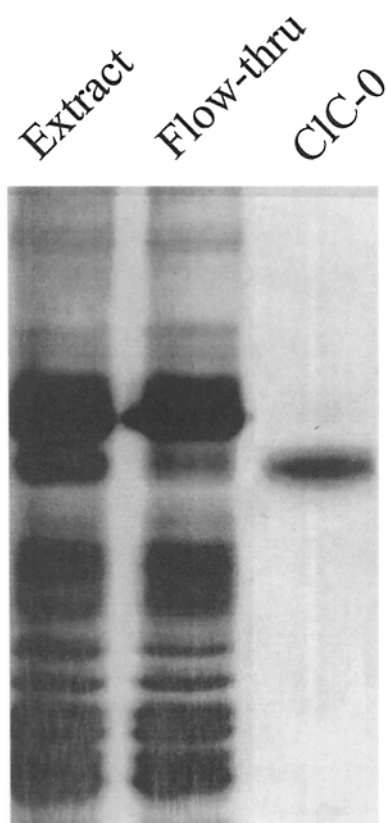
plex is constructed as a homodimer of the $\sim$90kD ClC-0 protein, with no associated "helper-subunits" (Middleton et al., 1994*b*; but see Steinmeyer et al., 1994, for an argument that the active channel is a homotetramer).

External Cl⁻ Affects ClC-0 Gating by Two Mechanisms

External Cl⁻ promotes the opening of ClC-0 (Pusch et al., 1995). The large magnitude of this effect is apparent in Fig. 3, which shows a steady-state macroscopic record in a lipid bilayer containing $\sim$500 reconstituted ClC-0 channels held at -50 mV, initially in symmetrical 150 mM Cl⁻ solutions. Lowering external Cl⁻ from 150 to 25 mM results in a profound reversible inhibition of inward current. Since this maneuver substantially increases the driving force for anion permeation at the negative holding voltage, the reduction in macroscopic current must be due to a decreased probability of channel opening. The single-channel records of Fig. 4, taken at fixed voltage and varying external Cl⁻, confirm this expectation. Increasing external Cl⁻ concentration activates the channel by two separate mechanisms. At high external Cl⁻ (150 mM), inactivation events are quite infrequent and short-lived, but they become far more prominent and long-lived when external Cl⁻ is reduced to 4 mM. The figure further shows that the fast-gating process is also affected, with decreased external Cl⁻ leading to lower open probability within the burst. Thus, Cl⁻ both antagonizes the appearance of the slow inactivated state and promotes rapid activation gating. Our experiments below focus solely on the influence of Cl⁻ and voltage on fast activation gating.

FIGURE 2. Preparation of purified of ClC-0. ClC-0 was prepared by immunoaffinity procedures, and samples at three different stages during the preparation are displayed on silver-stained 7.5% polyacrylamide gels.
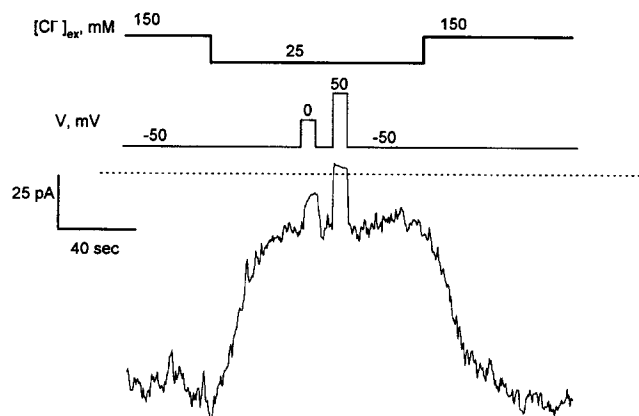

FIGURE 3. Effect of external Cl⁻ on macroscopic ClC-0 current. Approximately 500 ClC-0 channels were incorporated into a lipid bilayer by fusion of *Torpedo* electroplax plasma membrane vesicles. After current stabilized at a holding potential of -50 mV with symmetrical 150 mM Cl⁻, external Cl⁻ was reduced to 25 mM, as indicated. Voltage was briefly changed to 0 and 50 mV where indicated, and then external Cl⁻ was returned to 150 mM. Dashed line shows level of zero current.

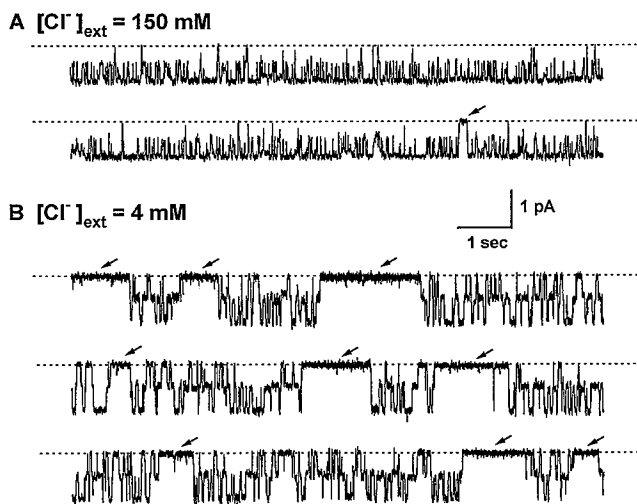**A** [Cl⁻]_ext = 150 mM

B [Cl⁻]_ext = 4 mM

| 1 pA
| 1 sec

FIGURE 4. External Cl⁻ affects both fast activation and slow inactivation gating. Continuous recordings of single channels were collected at either symmetrical 150 mM Cl⁻ (*A*) or 4 mM external Cl⁻/150 mM internal Cl⁻ (*B*). Dashed lines represent nonconducting level of current, and arrows indicate inactivation events. Holding potential was −50 mV.

Steady-state Open Probability Depends on External Cl⁻

The single-channel traces of Fig. 5 show in detail the activation of fast gating of ClC-0 by external Cl⁻. In these records, voltage and internal Cl⁻ were held fixed at −60 mV and 150 mM, respectively, while external Cl⁻ was changed from 1 to 150 mM. At each Cl⁻ concentration, dwell-times were exponentially distributed and the frequencies of appearance of the three fast-gating states rigorously followed binomial distributions. From records like these, we may derive voltage-activation
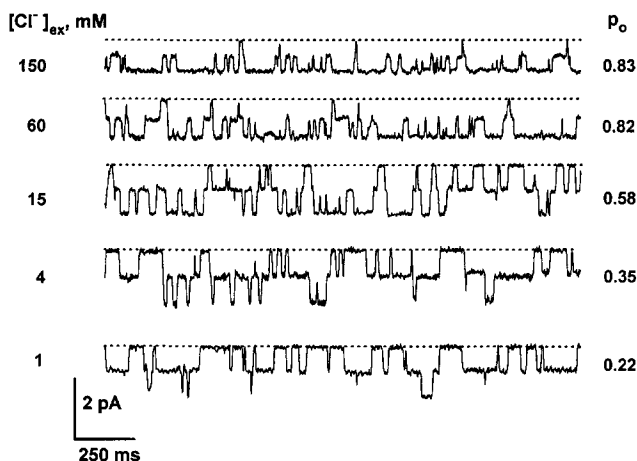
[Cl⁻]_ex, mM

[Cl⁻]_ex, mM		P_o
150		0.83
60		0.82
15		0.58
4		0.35
1		0.22

2 pA

250 ms

FIGURE 5. Effects of external Cl⁻ on activation gating of ClC-0. Representative segments are shown for single-channel records taken at −60 mV and 150 mM internal Cl⁻, with external Cl⁻ concentrations indicated. Open probability calculated for 30–60 s of each record is shown at the right of each trace. Each record is taken from a separate channel.

curves at different Cl⁻ concentrations (Fig. 6). The voltage dependence of open probability follows conventional expectations, with an effective gating charge of ∼1.0, a voltage dependence four- to eightfold lower than values typically found for voltage-gated cation channels. In all cases, open probability approaches unity (>0.99) at very depolarized potentials. As external Cl⁻ increases, the voltage activation curve shifts to the left along the voltage axis without significant change in apparent gating charge. This shift is due specifically to Cl⁻, since we obtained similar results whether or not we held ionic strength constant by replacing Cl⁻ with glutamate (data not shown). These measurements of absolute open-probability corroborate the effects of Cl⁻ described on macroscopic ClC-0 currents expressed in *Xenopus* oocytes (Pusch et al., 1995). Moreover, they point up an additional feature of activation gating: incomplete closure of the channel at very large negative potentials. The channel open-probability appears to approach a nonzero asymptote (∼0.15 under these conditions) at highly negative voltages. As we shall see later, this behavior in the strongly hyperpolarized region is informative in distinguishing among various models for voltage and Cl⁻ activation.

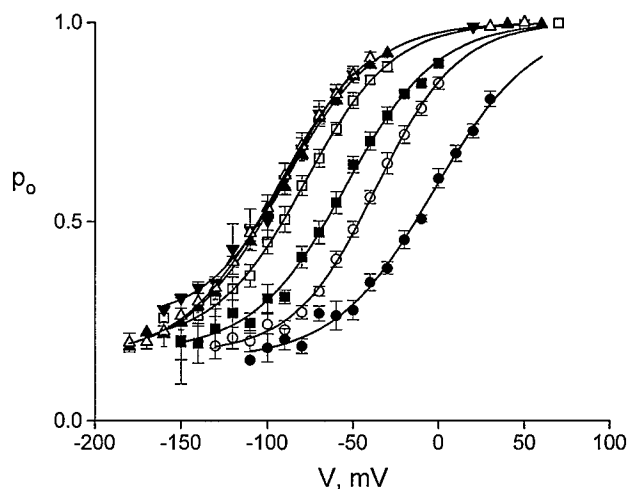As external Cl⁻ is lowered below 150 mM, the voltage activation curve shifts progressively to the right, ∼40

FIGURE 6. Steady-state voltage-activation curves for ClC-0 at varying external Cl⁻. Channel open probability, p_o, was measured as a function of voltage at different external Cl⁻ concentrations. Each point represents mean ± SE of 3–10 separate determinations in different bilayers; points without error bars represent means of duplicate determinations. Solid curves were drawn according to a simple voltage-dependent equilibrium:

$$p_o = p_{min} + (1 - p_{min}) / [1 + \exp(-zF(V - V_o)/RT)],$$

with $p_{min} = 0.16$–0.2 and $z = 0.9$–1.1. External Cl⁻ concentrations in mM and half-activation voltages, V_o, in mV, were: (●) 1, −3; (○) 4, −37; (■) 15, −55; (□) 60, −79; (▲) 150, −93; (△) 300, −95; (▼) 600, −88; internal Cl⁻ was 150 mM in all cases.

mV per 10-fold change of Cl⁻. No data below 1 mM Cl⁻ are reported here, since channels became quite unstable under such conditions; but in a few attempts to reduce Cl⁻ even further, we observed the activation curve to continue this rightward trend. In contrast, the position of the activation curve saturates at high Cl⁻; the half-saturation voltages at 150, 300, and 600 mM Cl⁻ are not significantly different (−93, −95, and −88 mV, respectively). These observation confirm the proposal of Pusch et al. (1995) that a Cl⁻ binding site accessible from the external solution is involved in controlling channel gating. Following the finding that conducting anions shift the activation curve in parallel to their permeation characteristics, these workers argued that the regulatory site is located in the conduction pathway of ClC-0.

Opening Rate Is Strongly Influenced by External Cl⁻

To obtain a more detailed picture of the Cl⁻ effect on ClC-0, we examined single-channel gating kinetics. The channel opening rate, α, depends on both voltage and Cl⁻ concentration (Fig. 7). It is clear that at a fixed Cl⁻ concentration, the opening rate is not a simple exponential function of voltage. At depolarized potentials, the opening rate increases exponentially with voltage, with an effective gating charge of ∼0.7 and no indication of a maximum value at depolarized voltages. With increasing hyperpolarization, however, the opening rate exhibits a striking and unusual behavior: a nonmonotonic variation with voltage. The opening rate displays a minimum at very negative potentials; this behavior can be seen more clearly with data analyzed from individual channel records (Fig. 8) than from values
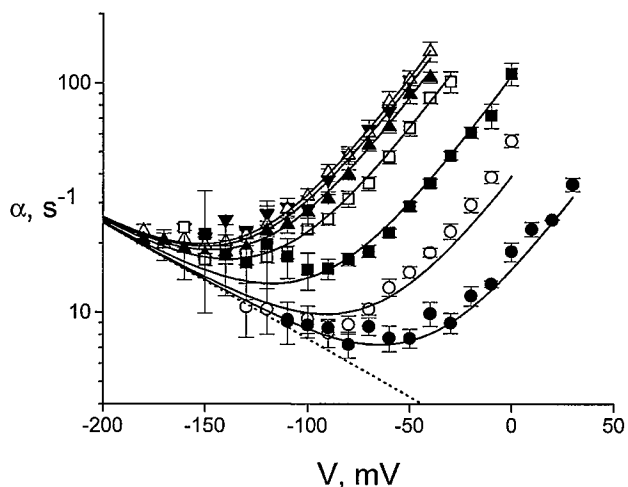

FIGURE 8. Direct observation of nonmonotonic voltage dependence. A single channel was recorded at 1 mM external Cl⁻ and 150 mM internal Cl⁻ at the three holding voltages indicated. Data segments within bursts are shown, with no inactivation events present. Dashed lines display the state-0 level.

averaged among several single channels. In these traces, it is apparent that the state-0 dwell-times are longer, on average, at −70 mV than at −20 mV, as expected from the decrease of opening rate as voltage is made more negative. However, as voltage is made more negative still (−110 mV), the state-0 dwell-times shorten, in contradiction to conventional expectations. This reversal of voltage dependence in the opening rate is seen across the entire range of Cl⁻ concentrations, even at saturating levels of Cl⁻. Viewed as a whole, the opening rate data all fall above an asymptotic lower envelope (dashed line, Fig. 7) with a reversed voltage dependence (apparent gating charge ∼−0.3).

The Closing Rate Is Weakly Dependent on Voltage and External Cl⁻

The channel's closing rate is also sensitive to voltage and external Cl⁻, but less so than the opening process, as shown in Fig. 9. The closing rate decreases exponentially with depolarization across the entire voltage range, with effective gating charge of ∼−0.4. Increasing external Cl⁻ from 1 to 600 mM decreases the value of the closing rate by only a small factor (∼2) at all voltages. Thus, while the open probability's voltage dependence is determined by both the opening rate and the closing rate, its external Cl⁻ dependence derives almost completely from an effect on opening.

Internal Cl⁻ Effects

We also carried out a few experiments varying internal Cl⁻ while holding external Cl⁻ fixed at 150 mM. These experiments are limited because this low-conductance channel gates at negative voltages, near the Cl⁻ reversal potential at low internal Cl⁻, where the single-channel current is very small. Results with internal Cl⁻ from 60 to 300 mM are shown in Fig. 10. In contrast to the effect of external Cl⁻, a reduction of internal Cl⁻ concentration lowers the opening rate only a small amount (Fig. 10 A), particularly at more hyperpolarized potentials; however, lowering the Cl⁻ concentration in-

FIGURE 7. Dependence of ClC-0 opening rate on external Cl⁻. Single-channel records were collected in 3–10 separate bilayers under conditions of Fig. 6, and opening rate constants α were calculated according to Eq. 2b. Symbols are as in Fig. 6. Solid curves are drawn according to Eq. 9, with parameters given in Table II. The dashed line represents the asymptotic voltage dependence of the channel at zero Cl⁻, Eq. 7a, with $\alpha_1(0)$ and z_1 given in Table II.
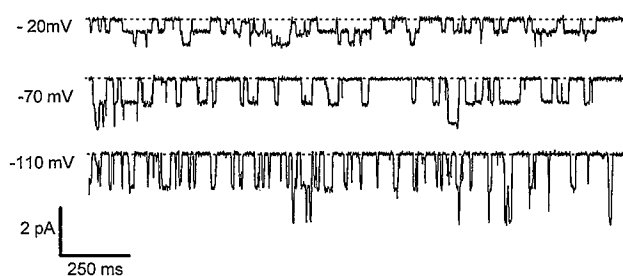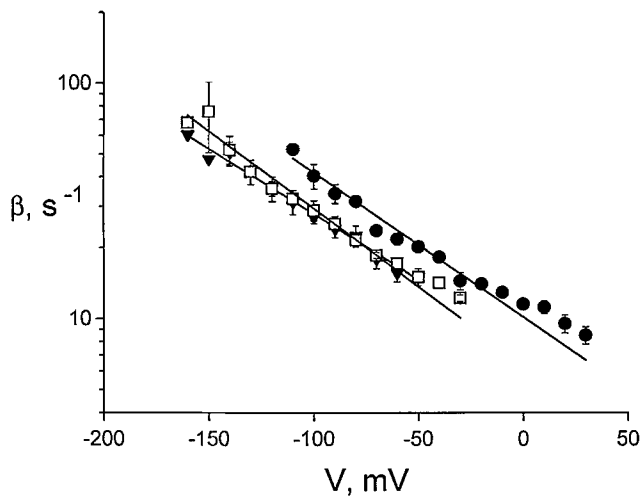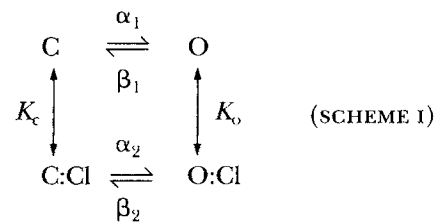
FIGURE 9. Closing rate of the ClC-0 channel is also voltage dependent. Closing rates of ClC-0 were calculated according to Eq. 2d in recording taken as in Fig. 6. Solid lines represent single exponentials, with gating charge in the range of -0.3 to -0.4. External Cl^- concentrations are: ($\bullet$) 1, ($\square$) 60, and ($\blacktriangledown$) 600 mM.

creases the closing rate substantially (Fig. 10 B), with a fivefold decrease in Cl^- concentration shifting the closing rate to the right along the voltage axis ~90 mV. As a result, increasing internal Cl^- shifts the steady-state voltage-activation curve (Fig. 10 C) to the left along the voltage axis, as with external Cl^-. But internal Cl^- exerts a more prominent effect on the degree of incomplete closure at hyperpolarized potentials, an effect not observed with external Cl^-. As internal Cl^- increases, so does the value of the p_o asymptote at negative voltage, p_{min}, with no change in the apparent gating charge (legend to Fig. 10 C). This effect of internal Cl^- would not be detected in conventional macroscopic current experiments, since the current remaining at high negative voltage is usually designated a leak to be subtracted out before calculating "relative open probability" (Pusch et al., 1995).

A Preliminary Gating Model

To evaluate the source of voltage dependence of channel gating, we followed the approach used by Moczydlowski and Latorre (1983) to identify the voltage-dependent steps in the activation of slowpoke-type Ca^{2+}-activated K^+ channels. Previous work on ClC-0 (Pusch et al., 1995) suggested strongly that the site at which Cl^- activates the channel is located somewhere within the conduction pore. We consider a minimal model of the channel in which four states can be distinguished: open and closed conformations, each of which may be empty or occupied by a Cl^- ion at a specific site in the conduction pathway:

$$
\begin{array}{ccc}
 & \alpha_1 & \\
C & \rightleftharpoons & O \\
 & \beta_1 & \\
K_c \updownarrow & & \updownarrow K_o \qquad \text{(SCHEME I)}\\
 & \alpha_2 & \\
C{:}Cl & \rightleftharpoons & O{:}Cl \\
 & \beta_2 & \\
\end{array}
$$

Here, external Cl^- is assumed to bind to a site in the closed channel in a rapid equilibrium (dissociation constant K_c); internal Cl^- is explicitly assumed to be unable to reach this site in the channel's closed conformation. Since this site is located in the anion conduction pathway, however, it becomes accessible to both internal and external Cl^- when the channel opens (equilibrium dissociation constant K_o). The rate constants for opening (α_1, α_2). and closing (β_1, β_2) are in general different for the Cl^--liganded and unliganded channel. The fact that Cl^- activates the channel implies that $\alpha_2 > \alpha_1$. This scheme predicts that the observed opening and closing rates are occupancy-weighted averages of α_1 and α_2 or of β_1 and β_2:

$$
\alpha = \alpha_1 P(C) + \alpha_2 [1 - P(C)] \tag{4a}
$$

$$
\beta = \beta_1 P(O) + \beta_2 [1 - P(O)] , \tag{4b}
$$

where $P(C)$ and $P(O)$ are the conditional probabilities of the activator site being unliganded, given that the channel is either closed or open. The steady-state open probability is:

$$
p_o = \alpha / (\alpha + \beta) . \tag{5}
$$

This model demands that as external Cl^- increases at a fixed voltage, the observed opening rate increases in a rectangular hyperbolic fashion from a minimum value of α_1 to a saturation value of α_2:

$$
\alpha = (\alpha_1 + \alpha_2 [Cl^-]_{ex}/K_c) / (1 + [Cl^-]_{ex}/K_c) \tag{6}
$$

In Fig. 11, we show that the predictions of Eq. 6 are fulfilled. At a given voltage, the opening rate increases in the expected saturating fashion as external Cl^- is raised. By fitting data points with Eq. 6, we obtained values for α_1, α_2, and K_c at each membrane potential in the range -110 to -50 mV. The results are striking (Fig. 12 A). Only the opening rates are voltage dependent, while the Cl^- dissociation constant is not. These facts are in precise contradiction to the speculation (Pusch et al., 1995) that Cl^- ion confers voltage depen-
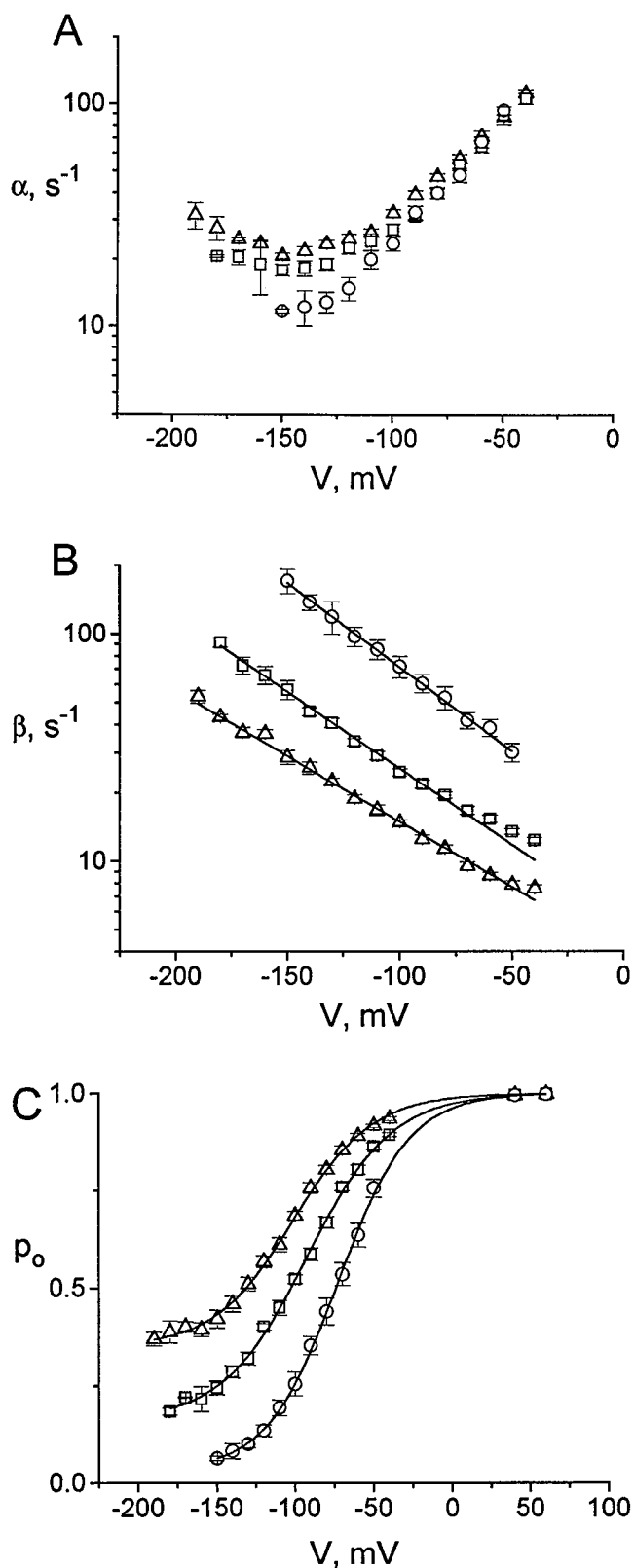
A

B

C

dence on ClC-0 gating by binding in a voltage-dependent fashion deep in the pore and that the conformational changes leading to channel opening do not involve any charge movement. Surprisingly, the voltage dependence of α_1 is of the opposite polarity to that of α_2, an unusual situation that explains the reversal of voltage-dependent opening at hyperpolarized potentials (Fig. 7) and the nonzero asymptote for open-probability at negative potentials (Fig. 6). Although we are concerned here with modelling activation only by external Cl$^-$, it is clear (Fig. 10 A) that the small effect of internal Cl$^-$ on the opening rate is seen only at highly negative voltages, where, as will be discussed below, the opening process is dominated by α_1.

DISCUSSION

Voltage dependence of ion channel gating has been traditionally viewed as arising from the movement through the transmembrane electric field of charged residues on the channel protein. In originally confronting this issue, Hodgkin and colleagues (Hodgkin et al., 1949; Frankenhaeuser and Hodgkin, 1957) considered the possibility that charge movement in Na$^+$ channels arises from ions in solution binding to sites within the membrane, but they quickly ruled out this idea. It is now understood (Larsson et al., 1996; Yang et al., 1996) that the S4 motif, a positively charged transmembrane sequence unique to the family of cation-conducting voltage-gated channels, acts as the voltage sensor in these proteins. Qualitatively, the ClC-0 Cl$^-$ channel appears to behave in the same manner, with depolarization speeding opening and retarding closing. However, no highly charged transmembrane sequences like S4 are found in ClC-type channels. Moreover, voltage dependence is not an unalterable, intrinsic property of this family of channels; while ClC-0 and ClC-1 show voltage dependent gating, for example, ClC-K1 and ClC-3 do not (Uchida et al., 1993; Kawasaki et al., 1994). Thus, the finding that extracellular Cl$^-$ promotes channel opening raised the interesting possibility that the permeant ion is itself the source of gating charge. Specifically, Pusch and colleagues (1995) suggested that extracellular Cl$^-$ accelerates channel opening by binding to a site within the conduction pore in the closed state, as though the site is located on the external side of a "gate." This binding step, which would be favored at more depolarized potentials, was pro-

FIGURE 10.   Effects of internal Cl$^-$ on the gating of ClC-0. Single-channel recordings were analyzed in which external Cl$^-$ was fixed at 150 mM, with internal Cl$^-$ at 60 mM (circles), 150 mM (squares), and 300 mM (triangles). Gating parameters plotted against membrane potential are: (A) Opening rate, α; (B) closing rate, β; (C)

open probability, p_o. Solid lines in B are single-exponential fits with slopes given in the text. Solid curves in C are fitted to conventional voltage-dependent gating curves, as in Fig. 6, with $z = 1.0$–1.1. Parameters of this fit are: $[Cl^-]_{in} = 60$ mM, $p_{min} = 0.03$, $V_o = -73$ mV; $[Cl^-]_{in} = 150$ mM, $p_{min} = 0.16$, $V_o = -93$ mV; $[Cl^-]_{in} = 300$ mM, $p_{min} = 0.35$, $V_o = -101$ mV.
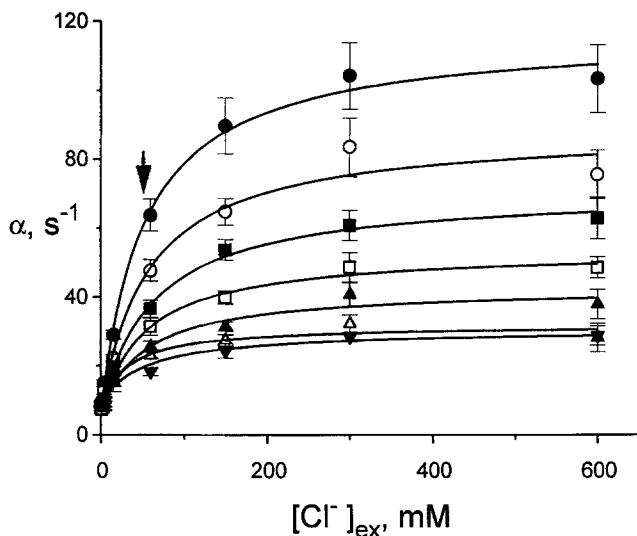
FIGURE 11. ClC-0 opening rate as a function of external Cl^-. The opening rates at membrane potentials from -110 to -50 mV were plotted as a function of $[CL^-]_{ex}$. Data points were fitted by an unweighted least-squares method according to Eq. 6, with parameters shown in Fig. 12 A. Voltages were, in mV: (●) -50, (○) -60, (■) -70, (□) -80, (▲) -90, (△) -100, (▼) -110. The arrow shows the average of values obtained for K_c on all plots.
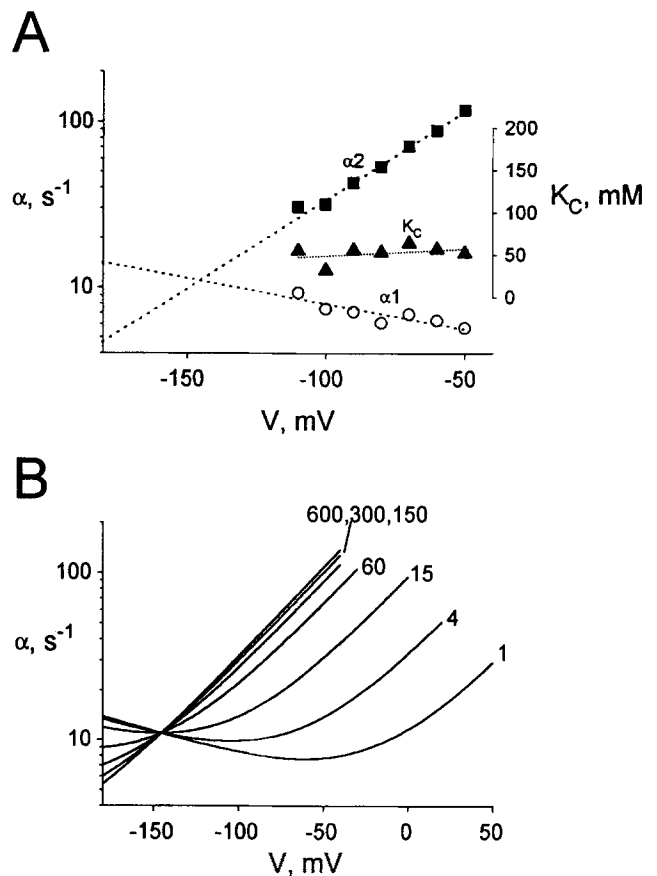

FIGURE 12. Opening rate analysis for four-state gating model. (A) Opening-rate parameters determined from data of Fig. 11 for the four-state model, SCHEME I, are shown. Effective gating charges are given in the text. (B) These parameters were used to calculate the general behavior of opening rate α expected for SCHEME I, at the indicated external Cl^- concentrations.

posed to produce all the voltage dependence of gating; the channel's conformational transitions were explicitly postulated to be voltage independent. It is our purpose here to test these ideas.

Four-state Gating Scheme

We first ask about the expectations of SCHEME I above, in which the Cl^- activation site is explicitly assumed to reside in the conduction pore. It is essential at the outset of the analysis to recognize that because the activator Cl^- is also a conducting ion, the gating of this channel is not at thermodynamic equilibrium, but rather is necessarily coupled to "downhill" transmembrane fluxes of Cl^-. For this reason, we cannot make any prediction for the behavior of the closing rate as Cl^- is varied, since binding and dissociation of Cl^- to the open channel represents ion conduction itself. The occupancy factor in Eq. 6, $P(O)$, reflects the detailed kinetic mechanism of ion conduction, and this is unknown. Likewise, the channel's steady-state open-probability, which in the standard view reflects the Gibbs free energy of the open-closed equilibrium, in this case is tainted by nonequilibrium components; for this reason the open-probability cannot be considered a fundamentally interpretable measurement. Because of the participation of dissipative Cl^- movements in the gating scheme, the usual "Boltzmann curve" is wholly inappropriate for describing voltage-dependent activation for this channel, except in a rough, empirical manner.

All is not lost, though, because the coupling of Cl^- binding to the opening rate does represent an equilibrium process, within the assumptions of SCHEME I. The anion readily gains access to the activator site from the external solution, but since the channel is closed, it cannot go through and must dissociate to the same side from which it came. The Cl^- binding processes are assumed to operate on the conduction timescale (<1 μs), much faster than gating (>1 ms). Thus, in order to analyze our results, we focus on the effects of Cl^- and voltage on the only mechanistically understandable parameter: the opening rate.

Our results (Fig. 11) demonstrate that Cl^- binding to the activation site is not voltage dependent. At each voltage tested, the opening rate increases in a rectangular hyperbolic fashion with external Cl^-. The value of the half-activation concentration, ~ 50 mM at all voltages tested, agrees well with the half-saturation concentration of the single-channel conductance (White and Miller, 1981). All the voltage-dependence of gating arises from the "conformational" rate constants. As

shown in Fig. 12 A, the opening-rate parameters, determined from Eq. 6, vary with voltage according to:

$$\alpha_1(V) = \alpha_1(0)\exp(z_1 FV/RT) , \qquad (7a)$$

$$\alpha_2(V) = \alpha_2(0)\exp(z_2 FV/RT) , \qquad (7b)$$

$$K_c(V) = K_c(0)\exp(z_c FV/RT) . \qquad (7c)$$

The effective gating charges are $z_1 = -0.18 \pm 0.04$, $z_2 = 0.62 \pm 0.02$, and $z_c = 0.08 \pm 0.09$.

While the Cl^- dissociation constant shows no significant voltage dependence, the behavior of the minimum and maximum opening rates is remarkable: they show opposite polarities of voltage dependence; α_1 decreases with depolarization while α_2 increases. This unusual behavior accounts for the complex, nonmonotonic voltage dependence of the opening rate. At relatively depolarized potentials, α_2 is large and dominates the opening rate; however, as the membrane potential is made increasingly negative, α_2 falls and α_1 increases, eventually determining the overall opening rate and reversing its voltage dependence. The challenge before us is to understand the physical meaning of these opposite voltage dependencies.

Failure of the Four-state Model

The four-state model (SCHEME I) works well in explaining the Cl^--dependence of the opening rate in the limited voltage range over which the analysis of Fig. 11 can be performed. However, it fails to account for our opening-rate data over the full range of voltage and Cl^- concentration (Fig. 7). There are two qualitative features of the data upon which the model fails, as indicated in Fig. 12 B, which plots the opening rates theoretically expected of the four-state model with parameters determined above; in fact, the problematic features are present in any four-state model in which $z_1 \neq z_1$. First, all such models demand a common point of intersection as Cl^- varies at the voltage where $\alpha_1 = \alpha_2$, as is apparent from Eq. 6. No such intersection point is seen in our data, but rather an asymptote towards which all curves converge at negative potentials. Second, all four-state models as in SCHEME I in which the Cl^- binding constant is voltage independent require a simple exponential dependence of α at saturating Cl^- concentrations. Our data at high Cl^- (150–600 mM), however, show a clear bending off at negative voltages, just as at lower Cl^-. Detailed analysis shows that these are fundamental, qualitative difficulties with the four-state model that cannot be patched up by parameter adjustment.

The inadequacy of SCHEME I arises from the fact that the opening rate of the Cl^--liganded channel fails to

become vanishingly small at very negative potentials, but instead levels off at a nonzero value. This might happen if there were a significant "polarizability" term in the voltage dependence of α_2, as has been speculatively proposed for other ion channels (Stevens, 1978). But the qualitative characteristics of our data—in particular, the rightward shift of the minimum point as Cl^- is lowered—violates the expectations of such an idea (analysis not shown). A more satisfactory fix is to modify SCHEME I by adding a second Cl^--liganded closed state (SCHEME II):
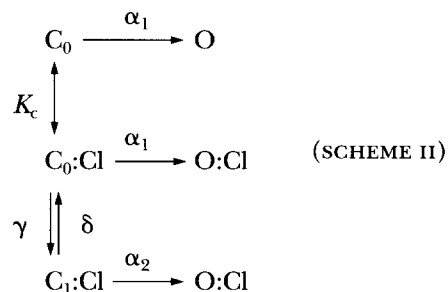
(SCHEME II)

In this scheme, C_0:Cl represents a closed, Cl^--liganded state from which a conformational change occurs to a new closed state, C_1:Cl, such that Cl^- ion is moved inwards into the voltage gradient. It is in this step that we postulate the significant charge movement of gating to occur, so that:

$$\gamma(V) = \gamma(0)\exp(z_\gamma FV/RT) . \qquad (8)$$

For simplicity, we explicitly propose that the charge movements for the opening steps are all the same, i.e., that $z_1 = z_2$. We also assume that Cl^- ion occupancy promotes the opening only of the C_1:Cl state, i.e., that both C_0 and C_0:Cl open with the same rate constant, α_1, and that $\alpha_2 >> \gamma$, δ, α_1 at all accessible voltages. In this way, γ is rate determining at depolarized voltages, but α_1 becomes rate determining at hyperpolarized voltage. We propose these restrictions in order to limit ourselves to a small set of parameters and, more importantly, to preserve the single-exponential distribution of the closed-state dwell-times. This limited three-closed-state model describes all of our data well (Fig. 7) over the entire range of voltage and Cl^- concentrations:

$$\alpha(V, [Cl^-]_{ex}) = \frac{\alpha_1(V) + [\alpha_1(V) + \gamma(V)][Cl^-]_{ex}/K_c}{1 + [Cl^-]_{ex}/K_c} . \qquad (9)$$

As in the discredited four-state model, α_1 shows a "reversed" voltage dependence, and K_c is without any voltage dependence at all. All opening rate data of Fig. 7 fall above an asymptotic dashed line with negative

slope; this line represents the pure opening rate of the channel $\alpha_1(V)$ in the C_o conformation. The solid curves in Fig. 7 are drawn with parameters given in Table II.

Cl^- Ion as the Gating Particle

This model offers a simple, intuitive picture of the collaboration of voltage and external Cl^- in opening the channel. First, we imagine that in the "C_0-closed" channel, a Cl^--binding site is located at the external end of the conduction pathway, so that the binding step feels none of the transmembrane voltage drop. Since the channel is closed, Cl^- is in rapid equilibrium with the external solution, and the occupancy of the site will depend only on external Cl^-, not on voltage. Both the liganded and unliganded channel open with the same rate constant; the opening transition involves a small amount of charge movement in the reversed direction, i.e., in which depolarization slightly accelerates closing ($z_1 \sim -0.3$). (We have no evidence as to the source of this reversed gating charge, whether it is intrinsic to the channel protein, or, perhaps, coupled to Cl^- movements from the internal solution.) Once liganded by Cl^-, however, the channel can undergo a conformational change to a different closed state, $C_1{:}Cl$. Once this $C_1{:}Cl$ state is attained, the channel opens immediately. The kinetic analysis shows that the charge movement conferring the major component of voltage dependence on the opening reaction resides in this step ($z_\gamma = 0.7$).

We further argue that the source of this charge is the Cl ion itself, moving inwards during the $C_o{:}Cl \rightarrow C_1{:}Cl$ transition, and not movement of charge intrinsic to the protein. If this transition involved intrinsic charge movement, similar charge movement would have to occur in analogous conformations of the Cl^--occupied open state, by the constraints imposed by thermodynamic cycles (Hanke and Miller, 1983). But if this were the case, depolarization would favor the charge-moved forms of both open and closed states, and the channel would not, in fact, be opened by depolarization. This problem does not apply, however, if Cl^- is the gating charge, since the conducting ion moves through the open channel, entering and leaving on both sides, and keeping the cycle under consideration above out of equilibrium.

It may seem awkward to postulate the physical movement of a pore-associated Cl^- binding site over halfway through the membrane voltage drop inside the closed channel, the crucial "γ-step" in this model. However, we could view this step more palatably if the conformational change alters the geometry of the pore, rather than physically moving the site, such that the voltage drop, falling over a longer segment of the channel protein, moves around the Cl^- ion (Jordan, 1986). This possibility, which we favor as more physically reasonable, is cartooned in Fig. 13.

We are at a loss to comment upon the behavior of the channel's closing rate other than superficially. Some of the voltage dependence of gating is involved in closing, but because of the nonequilibrium nature of Cl^- movements through the open state, we cannot identify the voltage-dependent steps. It is clear, though, that the closing process is not very sensitive to Cl^- ion on the external side of the channel. In contrast, increasing the
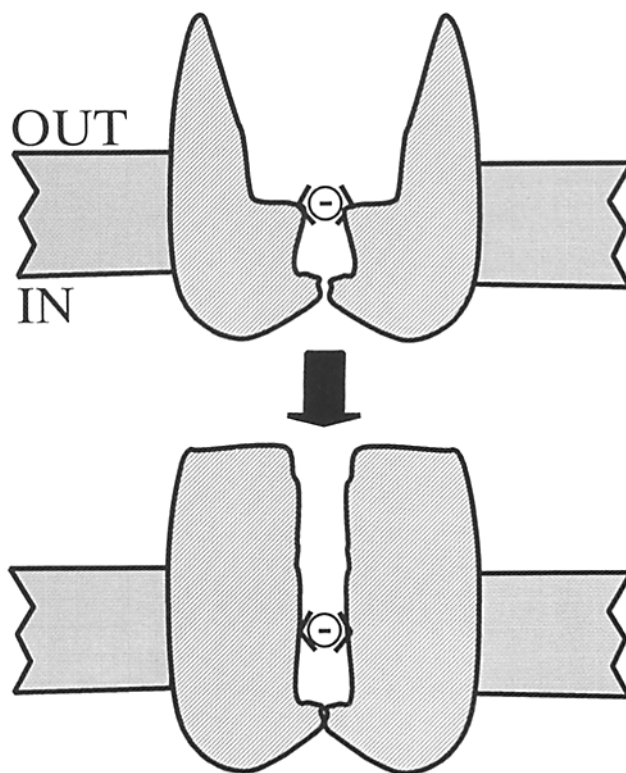

FIGURE 13. A possible interpretation of Cl^- as the gating charge of ClC-0. Cartoon shows a possible way in which bound Cl^- can act as the gating charge in the γ-step of SCHEME II. A conformational change in the closed channel is envisioned in which the pore narrows behind a bound Cl^- ion. This step involves a redistribution of the electric field within the pore and is electrically equivalent to the ion moving inwards, along the voltage drop.

TABLE II
Parameters for Curves in Fig. 7

Parameter	Value
$\alpha_1(0)$, s^{-1}	2.4
z_1	−0.29
$\gamma(0)$, s^{-1}	446
z_γ	0.7
K_i, mM	50

The Table reports the parameters used to generate the solid curves of Fig. 7 from Eqs. 7–9.

internal Cl^- concentration slows down the closing rate of the channel, recapitulating the "foot in the door" effect for voltage-dependent K^+ channels (Swenson and Armstrong, 1981). However, even this internal Cl^- effect on the closing rate is uninterpretable, since without detailed understanding on the permeation pathway, we can make no a priori predictions regarding open-channel occupancy by Cl^-.

Our picture of fast gating in ClC-0 is incomplete in several additional respects. The most serious deficiency is our reliance on the opening rate alone to produce a picture of charge movement in the channel. Channel opening reflects charge movement from the closed channel to a transition state between closed and open states; it does not refer to complete charge movement between closed and open states. Fortunately, most of the voltage dependence of the open probability is expressed in the opening rate, and so the qualitative conclusions derived from opening kinetics should apply to the overall gating process. Second, we have examined only the effects of Cl^- ion here, ignoring other conducting ions such as Br^- and NO_3^-, conducting anions also known to affect ClC-0 gating (Pusch et al., 1995). Finally, we have not yet derived a satisfactory explanation linking the nonequilibrium character of the fast gating process described here with the direct experimental violation of microscopic reversibility in ClC-0 in-

activation gating (Richard and Miller, 1990); we speculate that such a linkage must exist and, when understood, will provide deeper mechanistic insight into this channel's operation.

In summary, we have shown that ClC-0 gating responds to transmembrane voltage according to a novel mechanism unlike any seen in other voltage-gated channels. In the absence of external Cl^-, the conformational change leading to opening is weakly voltage dependent, and with reversed polarity; depolarization slows down closing rather than speeding it up, as though a small amount of "anti-gating charge" adventitiously moves upon channel opening. Activating Cl^- ion binds to the channel from the external solution in a voltage-independent way. We take this to mean that the binding site is located peripherally, close to the outside solution. In this Cl^--liganded state, the channel can open as above, displaying the reversed-polarity weak voltage dependence. Once Cl^- is bound, however, a conformational change to a second closed state may occur, and this step involves charge movement of ~ 0.7, as though the Cl^- ion itself, moving inwards, acts as the charge carrier. Once this new closed state is reached, the channel opens with a very high rate. Thus the speculation (Pusch et al., 1995) that Cl^- provides the gating charge for ClC-0, though exactly incorrect in detail, is exactly right in essence.

REFERENCES

Bauer, C.K., K. Steinmeyer, J.R. Schwarz, and T.J. Jentsch. 1991. Completely functional double-barreled chloride channel expressed from a single *Torpedo* cDNA. *Proc. Natl. Acad. Sci. USA.* 88:11052–11056.

Bryant, S.H., and A. Morales-Aguilera. 1971. Chloride conductance in normal and myotonic muscle fibres and the action of monocarboxylic aromatic acids. *J. Physiol. (Lond.).* 219:367–383.

Frankenhaeuser, B., and A.L. Hodgkin. 1957. The action of calcium on the electrical properties of squid axon. *J. Physiol. (Lond.).* 137:218–244

George, A.L., M.A. Carackower, J.A. Abdalla, A.J. Hudson, and G.C. Ebers. 1993. Molecular basis of Thomsen's disease (autosomal dominant myotonia congenita). *Nat. Genet.* 3:305–310.

Goldberg, A.F.X., and C. Miller. 1991. Solubilization and functional reconstitution of a chloride channel from *Torpedo californica* electroplax. *J. Membr. Biol.* 124:199–206.

Grunder, S., A. Thiemann, M. Pusch, and T.J. Jentsch. 1992. Regions involved in the opening of ClC-2 chloride channel by voltage and cell volume. *Nature (Lond.).* 360:759–762.

Hanke, W., and C. Miller. 1983. Single chloride channels from *Torpedo* electroplax: activation by protons. *J. Gen. Physiol.* 82:25–45.

Hodgkin, A.L., A.F. Huxley, and B. Katz. 1949. Ionic currents underlying activity in the giant axon of the squid. *Arch. Sci. Physiol.* 3:129–150

Jentsch, T.J., W. Gunther, M. Pusch, and B. Schwappach. 1995. Properties of voltage-gated chloride channels of the ClC gene family. *J. Physiol. (Lond.).* 482:19S–25S.

Jentsch, T.J., K. Steinmeyer, and G. Schwarz. 1990. Primary structure of *Torpedo marmorata* chloride channel isolated by expression cloning in *Xenopus* oocytes. *Nature (Lond.).* 348:510–514.

Jordan, P.C. 1986. Ion channel electrostatics and the shape of channel proteins. *In* Ion Channel Reconstitution. C. Miller, editor. Plenum Press, New York. 37–55.

Kawasaki, M., S. Uchida, T. Monkawa, A. Miyawaki, K. Mikoshiba, F. Marumo, and S. Sasaki. 1994. Cloning and expression of a protein kinase C-regulated chloride channel abundantly expressed in rat brain neuronal cells. *Neuron.* 12:597–604.

Larsson, H.P., O.S. Baker, D.S. Dhillon, and E.Y. Isacoff. 1996. Transmembrane movement of the Shaker K^+ channel S4. *Neuron.* 16:387–397.

Lloyd, S.E., S.H.S. Pearce, S.E. Fisher, K. Steinmeyer, B. Schwappach, S.J. Scheinman, B. Harding, A. Bolino, M. Devoto, P.

Goodyer, et al. 1996. A common molecular basis for three inherited kidney stone diseases. *Nature (Lond.)*. 379:445–449.

Middleton, R.E., D.J. Pheasant, and C. Miller. 1994a. Reconstitution of detergent-solubilized Cl⁻ channels and analysis by concentrative uptake of ^{36}Cl⁻ and planar lipid bilayers. *Methods (Orlando)*. 6:28–36.

Middleton, R.E., D.J. Pheasant, and C. Miller. 1994b. Purification, reconstitution, and subunit composition of a voltage-gated chloride channel from *Torpedo* electroplax. *Biochemistry*. 33:13189–13198.

Miller, C. 1982. Open-state substructure of single chloride channels from *Torpedo* electroplax. *Phil. Trans. R. Soc. Lond. B Biol. Sci.* 299: 401–411.

Miller, C., and E.A. Richard. 1990. The *Torpedo* chloride channel: intimations of molecular structure from quirks of single-channel function. *In* Chloride Transporters. A. Leefmans and J. Russell, editors. Plenum Press. New York. 383–405.

Miller, C., and M.M. White. 1980. A voltage-dependent chloride channel from *Torpedo* electroplax membrane. *Ann. NY Acad. Sci.* 341:534–551.

Moczydlowski, E., and R. Latorre. 1983. Gating kinetics of Ca^{2+}-activated K^+ channels from rat muscle incorporated into planar lipid bilayers. Evidence for two voltage-dependent Ca^{2+} binding reactions. *J. Gen. Physiol.* 82:511–542.

Neyton, J., and C. Miller. 1988. Potassium blocks barium permeation through calcium-activated potassium channels. *J. Gen. Physiol.* 92:549–567.

O'Neill, G.P., R. Grygorczyk, M. Adam, and A.W. Ford-Hutchinson. 1991. The nucleotide sequence of a voltage-gated chloride channel from the electric organ of *Torpedo californica*. *Biochim. Biophys. Acta.* 1129:131–134.

Palade, P.T., and R.L. Barchi. 1977. On the inhibition of muscle membrane chloride conductance by aromatic carboxylic acids. *J. Gen. Physiol.* 69:879–896.

Pusch, M., and T. Jentsch. 1994. Molecular physiology of voltage-gated chloride channels. *Physiol. Rev.* 74:813–825.

Pusch, M., U. Ludewig, A. Rehfeldt, and T.J. Jentsch. 1995. Gating of the voltage-dependent chloride channel ClC-0 by the permeant anion. *Nature (Lond.)*. 373:527–531.

Richard, E.A., and C. Miller. 1990. Steady-state coupling of ion-channel conformations to a transmembrane ion gradient. *Science (Wash. DC)*. 247:1208–1210.

Sigworth, F.J. 1994. Voltage gating of ion channels. *Q. Rev. Biophys.* 27:1–40.

Steinmeyer, K., R. Klocke, C. Ortland, M. Gronemeier, H. Jockusch, S. Grunder, and T.J. Jentsch. 1991a. Inactivation of muscle chloride channel by transposon insertion in mytotonic mice. *Nature (Lond.)*. 354:304–308.

Steinmeyer, K., C. Lorenz, M. Pusch, M.C. Koch, and T.J. Jentsch. 1994. Multimeric structure of ClC-1 chloride channel revealed by mutations in dominant myotonia congenita (Thomsen). *EMBO (Eur. Mol. Biol. Organ.) J.* 13:737–743.

Steinmeyer, K., C. Ortland, and T. J. Jentsch. 1991b. Primary structure and functional expression of a developmentally regulated skeletal muscle chloride channel. *Nature (Lond.)*. 354:301–304.

Stevens, C.F. 1978. Interactions between intrinsic membrane protein and electric field. An approach to studying nerve excitability. *Biophys. J.* 22:295–306.

Swenson, R.P., and C.M. Armstrong. 1981. K^+ channels close more slowly in the presence of external K^+ and Rb^+. *Nature (Lond.)*. 291:427–429.

Thiemann, A., S. Grunder, M. Pusch, and T.J. Jentsch. 1992. A chloride channel widely expressed in epithelial and non-epithelial cells. *Nature (Lond.)*. 356:57–60.

Uchida, S., S. Sasaki, T. Furukawa, M. Hiraoka, T. Imai, Y. Hirata, and F. Marumo. 1993. Molecular cloning of a chloride channel that is regulated by dehydration and expressed predominantly in kidney medulla. *J. Biol. Chem.* 268:3821–3824.

White, M.M., and C. Miller. 1979. A voltage-gated anion channel from electric organ of *Torpedo californica*. *J. Biol. Chem.* 254: 10161–10166.

White, M.M., and C. Miller. 1981. Probes of the conduction process of a voltage-gated chloride channel from *Torpedo* electroplax. *J. Gen. Physiol.* 78:1–19.

Wonderlin, W.F., A. Finkel, and R.J. French. 1990. Optimizing planar lipid bilayer single-channel recordings for high resolution with rapid voltage steps. *Biophys. J.* 58:289–297.

Woodbury, D.J., and C. Miller. 1990. Nystatin-induced liposome fusion. A versatile approach to ion channel reconstitution into planar bilayers. *Biophys. J.* 58:833–839.

Yang, N., A.L. George, and R. Horn. 1996. Molecular basis of charge movement in voltage-gated sodium channels. *Neuron.* 16: 113–122.